SAR IMAGE SEGMENTATION WITH ACTIVE CONTOURS AND LEVEL SETS

Ismail Ben Ayed, Carlos Vázquez, Amar Mitiche and Ziad Belhadj

Institut National de la Recherche Scientifique, INRS-EMT
Place Bonaventure, 800 de la Gauchetière West, Suite 6900
Montreal QC, H5A 1C6, Canada
e-mail: [benayedi,vazquez,mitiche]@inrs-emt.uquebec.ca
ziad.belhadj@supcom.rnu.tn

ABSTRACT

Automatic interpretation of synthetic aperture radar (SAR) images requires automatic segmentation of these images. Image segmentation is a fundamental problem in computer vision, particularly difficult with SAR images because of the presence of strong, multiplicative speckle noise. The purpose of this study is to investigate a novel algorithm for segmenting a synthetic aperture radar (SAR) image into a fixed but arbitrary number of Gamma-homogeneous regions. This unsupervised algorithm is based on active contours and consists in evolving closed simple planar curves to minimize a criterion containing a term of conformity of data to a model of SAR image intensity and a term of regularization. The curve evolution equations are implemented via level sets for numerical stability and to allow variations in the topology of the curves during their evolution. Examples are given using real SAR images.

1. INTRODUCTION

Segmentation is a fundamental problem in synthetic aperture radar (SAR) image automatic interpretation. Due in part to the presence of speckle, which can be modeled as strong, multiplicative noise, segmentation of SAR images is generally acknowledged as a difficult problem. This problem has been widely studied and a large number of methods have been proposed. By and large, most of these methods implement traditional views of segmentation based on schemes such as contour detection, histogram thresholding, and region growing, with a particular concern for proper modeling of speckle [1] [2] [3] [4] [5]. Such schemes instantiate mostly local operations and thus lack the robustness and tractability of recent variational methods, particularly those based on curve evolution and level sets which have been applied mainly to optical images [6] [7] [8] [9] [10] [11]. For SAR images, a classical snake model [12] is used in [13] [14]. In this region-based scheme, a contour is iteratively deformed to locate the boundary of the object, guided by a statistical criterion and it was shown to improve the traditional LR filter. The classical active contour model presents, however, several limitations. In particular, it is sensitive to initial contour placement and, most importantly, it cannot handle topological changes of the curves during their evolution. In this study, we use active curve evolution via level sets [15] to segment SAR images into a fixed but arbitrary number N of Gamma-homogeneous regions. Level-sets have the significant advantage of allowing, in a natural and numerically stable manner, variations in the topology of active curves. We first present a SAR image model representative of speckle noise. A two-region active contour evolution formulation and its level set representation is then described that uses this model. Finally, we extend the formulation to multiregion segmentation by stating the N-region segmentation problem as a minimization of $N-1$ two-region energy functionals. Examples on synthetic and real SAR images are given.

This study was supported in part by the Natural Science and Engineering Research Council of Canada under grant OGP0004234.

2. FORMULATION

Let $I : \Omega \rightarrow \mathbb{R}^n$ be the intensity SAR image to be segmented, defined on $\Omega \subset \mathbb{R}^2$. The goal of the segmentation process is to derive a partition of the image domain from the image I, i.e., a family $\mathcal{R} = \{\mathbf{R}_i\}_{i\in[1,N]}, \mathbf{R}_i \subset \Omega$ of N subsets of Ω such that they are pairwise disjoint $\mathbf{R}_i \cap \mathbf{R}_j|_{\forall i\neq j} = \emptyset$ and cover the image domain, $\cup_{i=1}^{N}\mathbf{R}_i = \Omega$, each region being homogeneous with respect to some image characteristics. We model the image in each region $\mathbf{R}_i, (i \in [1, N])$ by a Gamma distribution of mean intensity μ_i and number of looks L:

$$P_{\mu_i,L}(I(\mathbf{x})) = \frac{L^L}{\mu_i\Gamma(L)}\left(\frac{I(\mathbf{x})}{\mu_i}\right)^{L-1} e^{-\frac{LI(\mathbf{x})}{\mu_i}} \qquad (1)$$

The image in each region $\mathbf{R}_i, (i \in [1, N])$ is, therefore, characterized by its mean μ_i and the number of looks L, which we take to be the same for all regions.

2.1. Two-region segmentation

In this section, we consider the problem of segmenting an image into two regions. The formulation to be presented will subsequently be generalized to segmentation into a fixed but arbitrary number of regions.

Let $\mathbf{R}_1$ and $\mathbf{R}_2 = \mathbf{R}_1^c$ be a partition of the image domain into two regions. Assuming that $I(\mathbf{x})$ is independent of $I(\mathbf{y})$ for $\mathbf{x} \neq \mathbf{y}$, the problem is to determine the regions which maximize the likelihood:

$$\mathcal{L}(\mathbf{R}_1, \mathbf{R}_2|I) = \prod_{\mathbf{x}\in\mathbf{R}_1} P_{\mu_1,L}(I(\mathbf{x})) \prod_{\mathbf{x}\in\mathbf{R}_2} P_{\mu_2,L}(I(\mathbf{x})) \qquad (2)$$

Maximizing $\mathcal{L}$ is equivalent to minimizing $-\log(\mathcal{L})$. If we estimate μ_i by the average of I inside $\mathbf{R}_i$, $i = 1, 2$, i.e., if we take:

$$\mu_i = \frac{\int_{\mathbf{R}_i} I(\mathbf{x})\, d\mathbf{x}}{\int_{\mathbf{R}_i} d\mathbf{x}} \qquad i = 1, 2 \qquad (3)$$

0-7803-8554-3/04/$20.00 ©2004 IEEE.

then, using model (1), and following some algebraic manipulations, we obtain:

$$-\log(\mathcal{L}(\mathbf{R}_1, \mathbf{R}_2|I)) = L(a_1 \log \mu_1 + a_2 \log \mu_2) + c \quad (4)$$

where c is a constant which depends only on the image and the number of looks and, therefore, is independent of the segmentation, and a_i is the area of $\mathbf{R}_i$ $i = 1, 2$:

$$a_i = \int_{\mathbf{R}_i} d\mathbf{x} \qquad i = 1, 2 \quad (5)$$

The problem to solve becomes to determine $\mathbf{R}_1$, with $\mathbf{R}_2 = \mathbf{R}_1^c$, to minimize

$$\mathcal{D} = a_1 \log \mu_1 + a_2 \log \mu_2 \quad (6)$$

This criterion is the same as defined by the LR filter for edge detection and used in [5] to merge regions. We note that the means and areas depend on the segmentation and, consequently are to be estimated along with the segmentation process by (3) and (5).

2.1.1. *Solution by curve evolution*

To solve the problem stated by Eq. (6), we consider a simple closed planar curve $\vec{\gamma}(s) : [0, 1] \rightarrow \Omega$ parameterized by arc parameter $s \in [0, 1]$, and we associate its interior to region $\mathbf{R}_1$: $\mathbf{R}_1 = \mathbf{R}_{\vec{\gamma}}$. The Euler-Lagrange descent equations corresponding to $\mathcal{D}$ is obtained by embedding the curve $\vec{\gamma}$ into a family of one-parameter curves $\vec{\gamma}(s, t) : [0, 1] \times \mathbb{R}^+ \rightarrow \Omega$ and solving the partial differential equation:

$$\frac{d\vec{\gamma}}{dt} = -\frac{\partial \mathcal{D}}{\partial \vec{\gamma}} \quad (7)$$

where $\frac{\partial \mathcal{D}}{\partial \vec{\gamma}}$ denotes the functional derivative of the functional $\mathcal{D}$ with respect to the curve $\vec{\gamma}$. The segmentation is defined by the region $\mathbf{R}_1$ at convergence, i.e, when $t \rightarrow \infty$. We have:

$$\begin{aligned} \frac{\partial \mathcal{D}}{\partial \vec{\gamma}} &= \frac{\partial (a_1 \log \mu_1 + a_2 \log \mu_2)}{\partial \vec{\gamma}} \quad (8) \\ &= \left(\log \mu_1 \frac{\partial a_1}{\partial \vec{\gamma}} + \frac{a_1}{\mu_1} \frac{\partial \mu_1}{\partial \vec{\gamma}} + \log \mu_2 \frac{\partial a_2}{\partial \vec{\gamma}} + \frac{a_2}{\mu_2} \frac{\partial \mu_2}{\partial \vec{\gamma}} \right) \end{aligned}$$

Using the result in [6] which shows that, for a scalar function f, the functional derivative with respect to curve $\vec{\gamma}$ of $\int_{\mathbf{R}_{\vec{\gamma}}} f(\mathbf{x}) d\mathbf{x}$ is $\frac{\partial}{\partial \vec{\gamma}} \mathcal{F}(\vec{\gamma}) = f(\mathbf{x}) \vec{n}(\mathbf{x})$, where $\vec{n}$ is the external unit normal to $\vec{\gamma}$, we have:

$$\frac{\partial a_1}{\partial \vec{\gamma}} = \vec{n} \qquad \frac{\partial a_2}{\partial \vec{\gamma}} = -\vec{n} \quad (9)$$

and, with $s_1 = \int_{\mathbf{R}_1} I(\mathbf{x})\, d\mathbf{x}$ and $s_2 = \int_{\mathbf{R}_2} I(\mathbf{x})\, d\mathbf{x}$, we also have:

$$\begin{aligned} \frac{\partial \mu_1}{\partial \vec{\gamma}} &= \frac{\partial}{\partial \vec{\gamma}} \left(\frac{s_1}{a_1} \right) = \frac{a_1 \nabla s_1 - s_1 \nabla a_1}{a_1^2} = \frac{(I - \mu_1)}{a_1} \vec{n} \\ \frac{\partial \mu_2}{\partial \vec{\gamma}} &= \frac{\partial}{\partial \vec{\gamma}} \left(\frac{s_2}{a_2} \right) = \frac{a_2 \nabla s_2 - s_2 \nabla a_2}{a_2^2} = -\frac{(I - \mu_2)}{a_2} \vec{n} \end{aligned} \quad (10)$$

Note that the rightmost minus signs in the equations above are due to the fact that $\vec{n}$ being the external unit normal to $\mathbf{R}_1$, the external unit normal to its complement $\mathbf{R}_2$ is $-\vec{n}$. By substituting Eqs. (9) and (10) into Eq. (8) and after some algebraic manipulations we arrive at the evolution equation for curve $\vec{\gamma}$:

$$\frac{d\vec{\gamma}}{dt} = -\left(\log \frac{\mu_2}{\mu_1} + I \frac{\mu_1 - \mu_2}{\mu_1 \mu_2} \right) \vec{n} \quad (11)$$

which will define the segmentation at convergence, i.e, when $t \rightarrow \infty$. To obtain a smooth solution curve and avoid the occurrence of small, isolated regions in the final segmentation, a regularization term, $\mathcal{R}$, is added to the data related functional $\mathcal{D}$. This term is often given in the terms of the length of the boundary of $\mathbf{R}_1$. For instance, $\mathcal{R}$ is often taken to be, in terms of $\vec{\gamma}$:

$$\mathcal{R} = \lambda \oint_{\vec{\gamma}} ds \quad (12)$$

where λ is a real positive constant. The derivative of $\mathcal{R}$ with respect to $\vec{\gamma}$ is:

$$\frac{\partial \mathcal{R}}{\partial \vec{\gamma}} = -\lambda \kappa \vec{n} \quad (13)$$

where κ is the mean curvature function of $\vec{\gamma}$. With this regularization term, the final evolution equation for $\vec{\gamma}$ is:

$$\frac{d\vec{\gamma}}{dt} = -\left(\log \frac{\mu_2}{\mu_1} + I \frac{\mu_1 - \mu_2}{\mu_1 \mu_2} + \lambda \kappa \right) \vec{n} \quad (14)$$

2.1.2. *Level-set implementation*

We use the level-set formalism [15] to implement the evolution Eq. (14). A level-set representation of curve evolution is much more efficient than an explicit representation which explicitly discretize $\vec{\gamma}$ using a set of points, as with classical snakes. Indeed, there are several problems with an explicit representation of $\vec{\gamma}$. First, curve topological changes, which occur during evolution, are difficult to effect. Second, the result depends strongly on the parameterization and small errors in the representation can be significantly amplified during evolution. In contrast, a level-set representation allows topology changes in a natural way, and can be implemented by stable numerical schemes. The idea is to represent implicitly curve $\vec{\gamma}$ as the zero level of a function $\phi : \mathbb{R}^2 \rightarrow \mathbb{R}$, i.e, $\vec{\gamma} = \{\mathbf{x} | \phi(\mathbf{x}) = 0\}$. One can show [15] that if the evolution of $\vec{\gamma}$ is described by the equation:

$$\frac{d\vec{\gamma}(s, t)}{dt} = F(\vec{\gamma}(s, t), t) \vec{n}(s, t) \quad (15)$$

where F is a real-valued function defined on $\mathbb{R}^2 \times \mathbb{R}^+$, the evolution equation of function ϕ, with the convention that $\phi > 0$ inside the zero level-set, is given by:

$$\frac{\partial \phi(t, \mathbf{x})}{\partial t} = F(t, \mathbf{x}) \|\vec{\nabla} \phi(t, \mathbf{x})\| \quad (16)$$

In our case, the level set evolution equation corresponding to (14) is given by:

$$\frac{\partial \phi}{\partial t} = -\left(\log \frac{\mu_2}{\mu_1} + I \frac{\mu_1 - \mu_2}{\mu_1 \mu_2} + \lambda \kappa \right) \|\vec{\nabla} \phi\| \quad (17)$$

The curvature is computed in terms of the level set function by:

$$\kappa = \operatorname{div} \left(\frac{\nabla \phi_i}{|\nabla \phi_i|} \right) \quad (18)$$

Discretization of level-set equation is detailed in [15]. We should note that this evolution equation is only valid for points on the curve $\mathbf{x} \in \vec{\gamma}$. However, we can extend this equation for the evolution of ϕ over Ω.

2.1.3. Examples of results

To verify the SAR image intensity model, and the two-region segmentation algorithm, we first use a synthetic image with speckle noise. It consists of two regions. One of the regions, which has two disjoint components, is to be segmented against the other by a single active curve the initial position of which is shown overlaid on the original image in Figure 1a. Figures 1b and 1c show an intermediate and the final position of the curve, Figure 1d displays the computed segmentation.

Fig. 2 illustrates the segmentation ability of the algorithm on an ERS-1 intensity 1-look real SAR image of an agricultural scene. Fig. 2a) shows the original image and the initial curve; b) and c) show two intermediate steps during the evolution of the curve; d) contains the final segmentation; e) is one of the regions of segmentation against a black background and f) the other region against a white background. This two-region segmentation example shows the ability of the algorithm to give accurate edge location although edges are not well defined because of the presence of speckle.

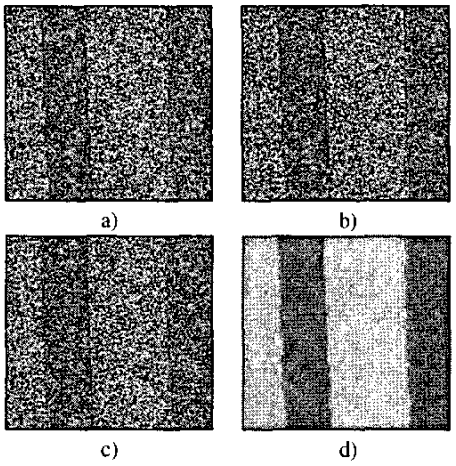

Fig. 1. Synthetic speckled image of 2 regions with $\rho = 1.7$ a) initialization, b),c) evolution and d) final segmentation.

2.2. Multiregion segmentation

To segment an image into several regions by means of active contours, we can assign a different contour to each region, and then allow each contour to evolve [8] [7] [10] [9]. Here, we follow our formulation in [9] and which we used to segment optical images. In [9], intensity in the regions of segmentation are modeled by Gaussians. Here, of course, and as in the two-region segmentation, we use the model described by (1), which is a more accurate model of image intensity with speckle noise.

Let $\vec{\gamma}_i|_{i=1,\ldots,N-1}$ be a family of curves, their interior defining regions $\mathbf{R}_i|_{i=1,\ldots,N-1}$. Region $\mathbf{R}_N$ will be formed by the intersection of the exteriors of all curves:

$$\mathbf{R}_N = \bigcap_{i=1}^{N-1} \mathbf{R}_i^c \tag{19}$$

We will derive a family of evolution equations for the curves $\vec{\gamma}_i, i = 1, \ldots, N-1$ to obtain, at convergence, a segmentation

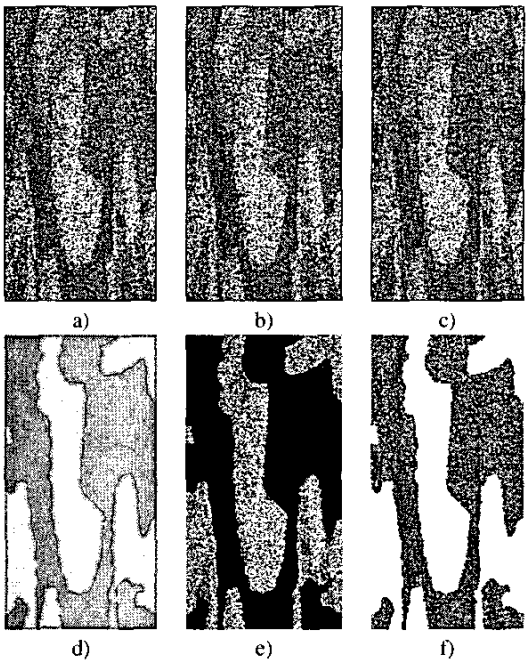

Fig. 2. A SAR image : two regions a) initialization; b) ,c) two steps in the curve evolution; d) final segmentation; e) one of the two regions of segmentation on black background; and f) the other region on white background.

into N regions, and the parameter of model (1) in each region, that best describe the SAR image. These evolution equations follow a formulation of image segmentation as a clustering problem under spatial constraints [9].

For simplicity of notation let $e_i(x) = -\log P_{\mu_i,L}(I(\mathbf{x}))$, $i = 1, ..., N-1$, where $P_{\mu_i,L}$ is the SAR intensity model defined in (1). Following the view of image segmentation as a problem of clustering under spatial constraints of the image intensity values, described by model (1) within each region of segmentation, we define $N-1$ energy functionals, each corresponding to a curve $\vec{\gamma}_i$:

$$\mathcal{E}_\Omega(\vec{\gamma}_i|\mathbf{I}) = \int_{\mathbf{R}_i} e_i(\mathbf{x})\, d\mathbf{x} + \int_{\mathbf{R}_i^c} \psi_i(\mathbf{x})\, d\mathbf{x} + \lambda \oint_{\vec{\gamma}_i} ds \tag{20}$$

where $\psi_i(\mathbf{x}) = \min_{j \neq i}(e_j(\mathbf{x}))$.

Segmentation of the image is obtained from the following set of simultaneous minimizations, each involving two regions, namely, the interior of a curve and its complement.

$$\begin{cases} \mathbf{R}_i &= \arg\min_{\mathbf{R}_i} \left(\mathcal{E}_\Omega(\vec{\gamma}_i|\mathbf{I})\right), \quad i \in [1, N-1] \\ \mathbf{R}_N &= \bigcap_{i=1}^{N-1} \mathbf{R}_i^c \end{cases} \tag{21}$$

The evolution equations of curves $\vec{\gamma}_i$, $i = 1, ..., N-1$, for the minimizations (21) are:

$$\frac{d\vec{\gamma}_i}{dt}(\mathbf{x})|_{\mathbf{x}\in\vec{\gamma}_i} = -\left(e_i(\mathbf{x}) - \psi_i(\mathbf{x}) + \lambda\kappa_i(\mathbf{x})\right)\vec{n}_i(\mathbf{x}) \tag{22}$$

and the corresponding level set equations are:

$$\frac{\partial \phi_i(\mathbf{x},t)}{\partial t} = -\left(e_i(\mathbf{x}) - \psi_i(\mathbf{x}) + \lambda\kappa_i\right)\|\vec{\nabla}\phi_i(\mathbf{x},t)\| \qquad (23)$$

2.2.1. Example of results

The multi-region segmentation method is illustrated on the high speckle noise 1-look real SAR image of an agricultural area, shown in Figure 3a. We segment the image into three regions (visual inspection indicates three regions). The initial curves (in red and green) are shown in 3a, and the curves at convergence in 3b. The computed segmentation into three regions is shown in 3c, and each of the three regions of segmentation in 3d, 3e, and 3f.

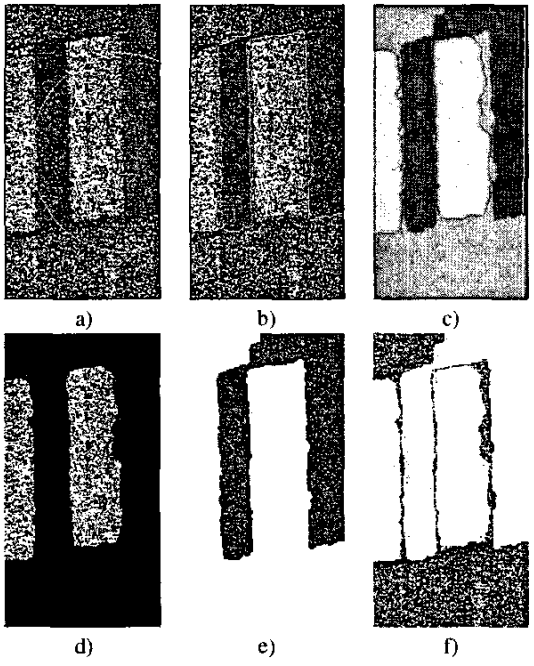

Fig. 3. A SAR image with three regions: a) original image and initial curves; b) the original images and the computed curves at convergence; c) computed segmentation; d), e), f) Each of the three regions of the computed segmentation.

3. CONCLUSION

We presented a curve evolution algorithm for segmenting a synthetic aperture radar (SAR) image into a fixed but arbitrary number of Gamma-homogeneous regions. This unsupervised algorithm is based on active contours and consists in evolving contours in order to minimize a criterion derived from a statistical framework. The evolution equations of contours were effected via level-sets evolution equations for a numerically stable implementation which allows changes in the topology of the curves during their evolution. The algorithm was illustrated on examples of segmentation of synthetic and real SAR images.

4. REFERENCES

[1] A. Bovik, "On detecting edge in speckle imagery," *IEEE Trans. Acoust. Speech Signal Processing*, vol. 36, no. 10, pp. 1618–1627, 1988.

[2] R. Tousi, A. Lopés, and P. Bousquet, "A statistical and geometrical edge detector for sar images," *IEEE Trans. Geosci. Remote Sensing*, vol. 26, no. 6, pp. 764–737, 1988.

[3] C. Oliver, I. M. Connell, and R. White, "Optimum edge detection in sar," in *SPIE on Satellite Remote Sensing*, Paris, 1995, vol. 2584, pp. 152–163.

[4] D. Smith, "Speckle reduction and segmentation of synthetic aperture radar images," *Int. J. Remote Sensing*, vol. 17, no. 11, pp. 2043–2057, 1996.

[5] R. Fjørtoft, A. Lopés, P. Marthon, and E. Cubero-Castan, "An optimum multiedge detector for sar image segmentation," *IEEE Trans. Geosci. Remote Sensing*, vol. 36, no. 3, pp. 793–802, 1998.

[6] S. Zhu and A. Yuille, "Region competition: Unifiying snakes, region growing, and bayes /MDL for multiband image segmentation," *IEEE Trans. Pattern Analysis and Machine intelligence*, vol. 18, no. 9, pp. 884–900, Sept. 1996.

[7] T. Chan and L. Vese, "Active contours without edges," *IEEE Trans. Image Processing*, vol. 10, no. 2, pp. 266–277, Feb. 2001.

[8] A. Yezzi, A. Tsai, and A. Willsky, "A fully global approach to image segmentation via coupled curve evolution equations," *Journal of Visiual Communication and Image Represnetation*, vol. 13, no. 1, pp. 195–216, Mar. 2002.

[9] C. Vazquez, A. Mitiche, and I. Ben Ayed, "Segmentation of vectorial images by a global curve evolution method," in *Proc. Reconnaissance de Forme et Intelligence Artificielle, RFIA-04*, Toulouse, France, Jan. 2004.

[10] A. Mansouri, A. Mitiche, and C. Vazquez, "Image segmentation by multiregion competition," in *Proc. Reconnaissance de Forme et Intelligence Artificielle, RFIA-04*, Toulouse, France, Jan. 2004.

[11] N. Paragios and R. Deriche, "Coupled geodesic active regions for image segmentation: A level set approach," in *Proc. European Conf. Computer Vision*, Dublin, Ireland, June 2000, pp. 224–240.

[12] M. Kass, A. Withkin, and D. Terzopoulos, "Snakes: Actives contours models," *Int. J. Computer Vision*, vol. 1, no. 1, pp. 321–333, Mar. 1988.

[13] O. Germain and P. Réfrégier, "Edge detection and localisation in sar images: a comparative study of global filtering and active contours approach," in *SPIE Europto Symposium on Remote Sensing*, Barcelona, sep 1998, vol. 3500, pp. 111–121.

[14] O. Germain and P. Réfrégier, "Edge location in sar images: performance of the likehood ratio filter and accuracy improvement with an active contour approach," *IEEE Trans. on Image Processing*, vol. 10, no. 1, pp. 72–78, Jan. 2001.

[15] J. Sethian, *Level Set Methods and Fast Marching Methods*, Cambridge University Press, 2 edition, 1999.